CHAPTER 7: MAP RELATIONSHIPS AND STRUCTURAL GEOLOGY.

The map included as Appendix 1 shows the geological relationships recorded in the field. The following description considers the structural phenomenon within each stratigraphical unit in order, followed by a description of the structural relationships existing between each of the stratigraphical units and the structural description of intrusive rocks.

7.1: Structures present within the basement gneiss:

Many of the ductile deformational features in the basement gneiss have been described in Chapter 2. However in addition to these ductile structures, several structures were recorded that suggest deformation under more brittle conditions (Chapter 2).

Whilst the true gneiss in the field area is generally banded (the foliation plane is partially defined by alternating quartzo-feldspathic and amphibolite lenses), outcrops along the southern strand of the Melinda Fault, bear little resemblance to the banded gneiss. Discrete amphibolite lenses are not present in these rocks, and no clear foliation is visible (Figure 7.1). The rocks consist of small, angular fragments of quartz (Figure 7.2), and are generally intruded by thin (<3mm) quartz-filled veins, locally at closely spaced intervals (Figures 2.14 and 7.3), which may give the appearance of foliation, especially as the trend of the quartz veins is generally parallel to the strike of the foliation planes in the banded gneiss (approximately E.N.E-W.S.W.) (Chapter 2). Locally, however, the quartz veins are not present. The lithology, in the absence of densely intruding veins, closely resembles a crush micro-breccia (as defined by Roering *et al.*, 1989) (Figures 2.13 and 7.1). These brittle fault rocks are intimately associated with the inferred position of the southern strand of the Melinda Fault, and may represent brittle reactivation of ductile fabrics.

In addition to these fault rocks, other brittle faults can be found locally within the basement rocks. These are generally characterised by low-angle fault planes, with slickenside lineations developed rarely on the planar surfaces (Figures 7.4 and 7.5). The orientation of the recorded surfaces are shown in Figure 7.6, which additionally

shows the orientation of slickenside lineations which were recorded on some of these planes. Slickenside lineations plotted in Figure 7.6 suggest that vergence along these faults is approximately towards the north or south.

7.2: Structures present within the Blouberg Formation:

Generally the Blouberg Formation is characterised by steeply-dipping and overturned bedding. The strata along the southern edge of Blouberg mountain generally dip southwards, with angles of dip between 45° and 90° (e.g. Figure 3.19). Locally these beds are overturned, and dip northwards at angles up to 55°. The steeply-dipping beds in the Blouberg area consist of strata of the Lower Member of the Blouberg Formation (Chapter 3). However, rare outcrops of the Upper Member in the Blouberg area have only gently-dipping beds, which are in contrast to the steeply-dipping bedding geometry of the Lower Member. The orientation of bedding planes shown in Figure 7.7 define an approximately horizontal E-W trending fold-axis. Such folding is also visible in smaller-scale folds throughout the outcrops of the Blouberg Formation (e.g. Figures 3.24 and 7.8).

Bedding orientations shown in Figure 7.9 were recorded from an outcrop of Blouberg strata at 23°05.76'S; 28°53.47'E (Figure 7.8). This outcrop is significant in that it is the only outcrop of Blouberg strata which was recorded to the north of the southern strand of the Melinda Fault (Section 3.3; Appendix 1). Comparison of Figures 7.7 and 7.9 shows that both outcrops of Blouberg strata have a similarly orientated fold-axis and deformational characteristics.

In comparison to the general southward or northward dip-direction of the Blouberg Formation in the Blouberg area, dip-directions of Blouberg strata in the Kranskop area have contrasting geometry. Both the Lower and Upper Members of the Blouberg strata have very steep dips (80°-90°), though here the dip direction is consistently to the east or west, in contrast to the consistent north-south dip in the Blouberg area (Figure 7.7).

Faulting is recorded only locally in the Blouberg Formation. Southward-verging thrust faults and more steeply-dipping, southward-verging reverse faults displace the

Blouberg strata (Figure 7.10a). The sense of movement of the fault (Figure 7.10a) can be gained from the measurement of slickenside lineations, which plunge 52°, and have a trend of 004° (dip-slip movement), and which exhibit stepping indicative of a reverse sense of movement. This fault does not cut the Mogalakwena Formation which unconformably overlies the Blouberg Formation (Figure 7.10a)(Section 7.7).

Similarly, basement gneiss is locally thrust over the Blouberg Formation at 23°07.17'S; 29°02.66'E, where the thrust is marked by the presence of a brittle fault rock, exhibiting a weak sub-horizontal foliation, with a dip-direction of 10°→030° (Figure 7.4). The vergence of this thrust fault may have been towards the south. At around 23°06.93'S; 28°58.17'E, and 23°07.96'S; 28°55.25'E, the thrusting of the basement over the Blouberg Formation can be inferred by the presence of basement topographically above only gently-dipping Blouberg strata (Appendix 1), and similarly may have been thrust with a southward vergence. Slickenside lineations, which are only rarely recorded from within the Blouberg Formation, are shown in Figure 7.11, which shows that such lineations are generally orientated along a north-south trend (Figure 7.12).

The presence of steep, southward-dipping bedding and northward-dipping overturned bedding, and the presence of small-scale southward-vergent reverse- and thrust faults can best be explained by the inferred presence of large-scale southward-vergent reverse- or thrust faults above each section of overturned strata (Figure 7.10b). In the Dantzig area (23°06.50'S; 29°01.50'E; Appendix 1), relatively horizontally bedded Blouberg strata underlie the southern side of the valley, whilst steeply-dipping and overturned Blouberg strata outcrop on the northern flank. The southern outcrops are locally overlain by basement rocks, and they appear to be separated from each other by a southward-vergent thrust. The northern strata may represent a duplication of Blouberg strata (a duplex structure) bound above and below (in the floor of the valley) by the large-scale thrust faults. Though no other duplex-type structures were recorded in the Blouberg Formation, the continued presence of steeply-dipping and overturned bedding attests to the presence of large-scale southward-vergent thrust faults affecting the Lower Member of the Blouberg Formation and the basement rocks throughout the Blouberg mountain area. Despite the relatively intense folding, and the inferred

presence of large-scale faults necessary to produce overturned beds typical of the Blouberg Formation, large portions of the Blouberg strata, though steeply-dipping or overturned, show little evidence for micro-to mesoscopic deformation, and as a result sedimentary structures are generally well-preserved.

7.3: Structures present within the Setlaole Formation:

The paucity of outcrops that can be correlated with the Setlaole Formation within the study area does not allow for ready determination of structures characteristic of the Setlaole strata. However the outcrops which could be correlated with the Setlaole Formation in the south-eastern part of the study area are characterised by generally horizontal or shallow dipping bedding planes, and a general lack of deformation.

Previously, Jansen (1976) suggested that the Blouberg Formation and Setlaole Formation may correlate, though Meinster (1977) argued against this correlation. Although the Setlaole and Blouberg Formations locally have comparable lithofacies (Chapter 3 and Section 4.2) the strong disparity between generally steeply-dipping and overturned strata of the Blouberg strata, and the gently-dipping or horizontally-inclined Setlaole strata, can be used as a means of discrimination between these two formations. If they are indeed correlated, it is difficult to reconcile the presence of intense deformation within the strata of the Blouberg Formation, without these structures being at least partially propagated in the Setloale Formation. Other characteristics (palaeocurrent trend and comparison of lithofacies) were also used in addition to structural characteristics to discriminate between the Blouberg and Setlaole Formations during mapping (Appendix 1).

7.4: Structures present within the Makgabeng Formation:

The Makgabeng Formation is comprised generally of facies of large-scale trough and planar cross-bedded sandstones, and bedding planes are rarely preserved. However, facies consisting of planar-bedded mudstones and sandstones indicate that there is little deformation present in rocks of the Makgabeng Formation. Dips of bedding planes reach a maximum of only 5°. As described in Chapter 6, dyke swarms locally intrude the Makgabeng Formation, generally along an E.N.E- W.S.W. trend. Locally

it seems that some of these dykes have intruded along pre-existing fault planes, as locally there seems to be small displacement of strata across these dykes, visible in vertical sections. Though these displacements appear to relate to dip-slip faulting, the precise sense of movement has proved difficult to establish.

The Makgabeng Formation is not developed in close proximity to the southern strand of the Melinda Fault, and as a result deformation associated with this fault was not recorded.

7.5: Structures present within the Mogalakwena Formation:

The southern and western outcrops of the Mogalakwena Formation are similar to the outcrops of the Makgabeng Formation in that there is a lack of evidence for much tectonic disturbance of the strata. Dips of bedding planes only rarely exceed 5°, and there is little evidence for faulting, either recorded in the field or visible on aerial photographs. However, in common with the Makgabeng Formation, dyke swarms with a general E.N.E.-W.S.W trend are intrusive into the Moglakwena strata (Appendix 1).

In contrast to the southern and western outcrops of the Mogalakwena Formation, outcrops exposed to the north and east are more likely to contain evidence for tectonic disturbance, especially in outcrops adjacent to the southern strand of the Melinda Fault. Here, the dip of bedding planes may locally reach 30° towards the south (Appendix 1), though generally dips of bedding planes remain low-angled, typical of the remainder of the Mogalakwena Formation.

Along the southern strand of the Melinda Fault, such as at areas around 23°07.40'S; 28°56.87'E and 23°07.30'S; 28°57.60'E, there are outcrops of small sets of trough cross-bedded sandstones with heavy mineral accumulations on foresests (Figure 4.66), which correlate well with the more distal outcrops of the Mogalakwena Formation (Section 4.4). These outcrops lie within and to the north of the southern strand of the Melinda Fault zone, and at two locations (23°07.60'S; 28°55.70'E and 23°07.10'S; 28°57.49'E), are juxtaposed against the more proximal, conglomeratic

facies of the Mogalakwena Formation. The two contrasting facies associations are locally developed only about 20m away from each other at comparable topographic heights, and can likely be explained by juxtaposition of the distal facies against the proximal facies by faulting. Narrow intervening areas between these two facies can locally be seen to be occupied by crush breccia (Section 7.1), or to be intruded by dykes (Appendix 1).

Mogalakwena strata (distal facies) to the north of the southern strand of the Melinda Fault are generally horizontally inclined, or reach only relatively low angles of dip (Appendix 1), and only rarely show evidence for faulting.

7.6: Structures present within the Sibasa and Wyllies Poort Formations:

The Sibasa Formation does not generally outcrop sufficiently well to establish any structures present within it. However, it can be noted that the present extent of both the Sibasa Formation and the Wyllies Poort Formation above, is restricted to the northern side of the southern strand of the Melinda Fault within the study area. No outcrops of the Sibasa or Wyllies Poort Formation were identified south of this fault.

The outcrop of the Wyllies Poort Formation is good in areas of high relief on Blouberg mountain, and towards the far north-eastern corner of the field area. In the area around Blouberg mountain, including areas adjacent to the southern strand of the Melinda Fault, the Wyllies Poort Formation exhibits horizontal to low-angled bedding planes (e.g. Figure 5.6), though the strata are typically intensely jointed (Figures 7.13 and 7.14). At least two sets of joints were recorded in the upper slopes of Blouberg mountain. The two approximately vertical joint sets strike at 260-280°, and at 355-035° though, wherever these two joint sets intersect, they have a consistent angular difference of 70-80°.

Locally the Wyllies Poort Formation is also cut by approximately east-west trending major faults (Appendix 1), which can be traced easily on aerial photographs, and which apparently have a dextral displacement, though only rarely are they apparent in the field. Small-scale faults, which are of parallel strike to the major faults cutting the Wyllies Poort Formation, were recorded locally. Rarely, these exhibit a fabric, such as

that shown in Figure 7.15, and generally indicate dextral movement. At 23°04.69'S; 28°59.49'E, in the steep cliffs of Wyllies Poort strata about half way up the preserved section, evidence was gained for bedding-parallel thrust-faulting. Drag folded joints developed on the lower fault plane, with slickensides developed (possibly by flexural slip) on the folded joint surfaces, suggest that the upper portion was moved towards 315° (Figure 7.16).

In contrast to the generally horizontal bedding of the Wyllies Poort Formation in the area bound by the southern and northern strands of the Melinda Zault zone, the Wyllies Poort strata adjacent to the northern strand of the Melinda Fault is highly tectonised. In the far north-eastern corner of the study area, several splays from the northern strand of the Melinda Fault, with approximately parallel strike, displace the Wyllies Poort Formation. Appendix 1 shows that, generally, these splays of the northern strand of the Melinda Fault have an apparent dextral displacement. Dips of bedding planes of the Wyllies Poort strata within the Fault zone locally approach 90° (Figure 7.17).

Areas of Wyllies Poort strata adjacent to one of the splays of the northern strand of the Melinda Fault zone are commonly strongly recrystallised, so that primary sedimentary structures are only rarely preserved. Additionally, the strata in this area are locally pervasively intruded by quartz-filled veins. Figure 7.18 shows an area at 23° 00.93'S; 29° 02.88'E, where veins strike 100°. At the same location, quartz-filled veins can be seen to have intruded along earlier brittle faults, as shown in Figure 7.19. Similarly, in Figure 7.20, a dilatational vein, which strikes 140°, indicates approximately 2cm of sinistral displacement during intrusion. In other areas, such as at 23°00.51'S; 29°07.71'E and 23°02.08'S; 28°59.78'E, veins are parallel to the strike of the northern strand of the Melinda Fault, and may reach widths of several metres (Figure 7.21). The location of the northern strand of the Melinda Fault at 23°03.02'S; 28°56.38'E is marked by a small hill (Figure 7.22), which is underlain by white quartzite, which may reflect total recrystallisation, and the intrusion by quartz veins, of earlier brecciated Wyllies Poort strata.

Evidence for the type of initial fault rock, which existed prior to recrystallisation or veining, can be gained locally where patches of Wyllies Poort strata have escaped recrystallisation. Figures 7.23 and 7.24 show planes of fault breccia which have not recrystallised, and thus it seems likely that the northern strand of the Melinda Fault was initially characterised by the presence of fault breccia along the numerous splays of the Fault zone, prior to recrystallisation. Fabrics in the fault rocks are only rarely preserved: Figure 7.25 shows a fault plane with a dip-direction of 83°→190°, which has a weak S-C fabric developed, which suggests a dextral sense of movement. Slickensides recorded within the fault have a trend of 100°, and a plunge of 0°.

The strike of joint planes recorded from areas adjacent to the northern strand of the Melinda Fault are shown in a rose diagram in Figure 7.26, which shows that joints generally strike N.W.-S.E, though are rather variable. The strike of veins recorded from this area are shown in a rose diagram in Figure 7.27, which show much variation, though again strike dominantly N.W.-S.E. The orientation of small-scale fault planes in the Wyllies Poort Formation are shown in Figure 7.28, which shows that the fault planes generally strike E.N.E.-W.S.W., and are steeply-dipping. Rarely, fault planes with low angles of dip are also recorded. Slickenside lineations, locally recorded on some of these fault planes, are shown in Figure 7.29, and indicate both dip-slip and oblique-slip displacement on steeply dipping fault planes. Lineations recorded on low-angled fault planes generally trend towards the N.W. In addition, the orientation of quartz crystal growth in veins could also be recorded rarely. These vein quartz crystals were found to have long axes trending 202° and 210°.

7.7: Relationships present between stratigraphic units in the study area:

This section will consider the relationships between each of the stratigraphic units in the study area, examining whether contacts are conformable, disconformable, nonconformable or unconformable.

The rocks which are considered as basement gneiss can be demonstrated to be nonconformably overlain by all of the sedimentary rocks discussed in previous chapters. Although the nonconformable contact between the gneiss and the Blouberg Formation cannot be seen due to cover, the location of the nonconformity can be

estimated within about 10m at 23°09.01'S; 28°42.01'E, at the base of the Kranskop river section. At locations such as 23°05.76'S; 28°53.47'E, folded Blouberg strata are recorded in close proximity to basement rocks. It is interesting to note, however, that despite the east-west trending fold axis in the Blouberg Formation, the foliation of the gneiss, which crops out less than 100m away, shows little evidence for having being folded, as the E.N.E. strike and vertical dip of the foliation planes remain comparable to those recorded from other areas.

Other locations where the basal beds of the Blouberg Formation can be seen occur at 23°07.39'S; 28°57.46'E, where the lower contact of vertically dipping Blouberg strata is separated from a crush breccia by a 5m-wide zone of jasperitic hydrothermal alteration. As shown in Chapter 2 and Section 7.1, this is more likely to represent a faulted contact, rather than a nonconformable relationship with the basement.

Though the Setlaole Formation could not be directly demonstrated to nonconformably overlie the basement, gneiss was recorded outside the field area just to the east of outcrops of the Setlaole Formation. Here, the basement rocks outcrop at comparable altitudes to the generally horizontally inclined Setlaole strata, and no other strata has been recorded in intervening areas. This suggests that the Setlaole Formation nonconformably overlies the basement. The Makgabeng Formation seems to be developed nowhere above the basement gneiss. The basal beds of the Makgabeng Formation, on the eastern side of the Makgabeng plateau can only be demonstrated to rest conformably on the Setlaole Formation at 23°16.50'S; 28°59.50'E. The Mogalakwena Formation at 23°05.58'S; 28°53.42'E can be directly observed overlying the basement, where the contact is marked by a thin (<20m) conglomerate with well-rounded quartz, quartzite and banded iron formation cobbles, typical of all Mogalakwena conglomerates. Whilst the Wyllies Poort Formation cannot be directly observed to rest non-conformably on the basement, it is most likely to do so around the eastern edge of Blouberg mountain (c. 23°05'S; 29°01'E). Here gneiss underlies areas of relatively high altitude (<1400m), just beneath the Wyllies Poort Formation, and no other strata have been recorded cropping out between the two lithologies.

The Mogalakwena Formation, in addition to its nonconformable relationship with the basement gneiss, can be demonstrated to be developed on a pronounced angular unconformity with the Blouberg Formation beneath. This relationship is best developed at 23°07.35'S; 28°57.53'E (Figure 7.30), 23°06.80'S; 28°59.40'E (Figure 7.31), 23°05.76'S; 28°53.47'E (Figure 7.32) and also at 23°09.12'S; 28°41.22'E, at the top of the Kranskop section. The basal beds of the Mogalakwena Formation in all cases are conglomeratic, though in the case of the outcrops at Varedig (Figure 7.32) and Kranskop, the conglomeratic strata are thin (about 20m) compared to the Mogalakwena strata south of the southern strand of the Melinda Fault, where the basal conglomeratic beds may be at least 90m thick (Section 4.4.1.1).

The Mogalakwena is generally regarded as having a conformable relationship with the Makgabeng Formation beneath (e.g. Callaghan *et al.*, 1991). The strongly contrasting nature of the well-sorted, medium-grained arenaceous Makgabeng Formation and the coarse-grained sandy and conglomeratic Mogalakwena Formation allow for ready identification of the contact between these two formations (Figure 7.33). However, outcrops on the Makgabeng Plateau (e.g. 23°16.39'S; 28°52.57'E), where the contact between the Makgabeng and Mogalakwena formations is well-exposed, show clear joint sets developed in the underlying Makgabeng Formation which are not propagated in the Mogalakwena Formation above (Figure 7.34), and which can locally be observed to be exploited by the Mogalakwena Formation as basal channel margins (Figure 7.35). In addition, reduction spots which can be seen to be developed on the upper surface of the Makgabeng Formation do not continue into adjacent Mogalakwena rocks (Figure 7.36). This indicates that the Makgabeng Formation had lithified prior to deposition of the Mogalakwena Formation. It was shown in Section 4.3.3 that the massive sandstone facies was developed generally in the upper half of the Makgabeng Formation, and is absent from the lower half. Thus, the presence of this facies provides a coarse reference for the stratigraphic height of an outcrop within the Makgabeng Formation. Although both the Makgabeng and Mogalakwena Formations are generally horizontally-bedded, indicating a disconformable relationship, the Mogalakwena Formation can only be demonstrated to be deposited above Makgabeng outcrops frequently containing the massive sandstone facies in the south of the field area. The massive sandstone facies could not be recognised in the Makgabeng strata below the Mogalakwena Formation in the

outcrops towards the north. This suggests that the Mogalakwena Formation may be developed on successively older Makgabeng strata towards the north, and thus represent a slight angular unconformity between these two formations of the Waterberg Group.

Although it has generally been regarded (e.g. Jansen, 1976; Meinster 1977; Brandl, 1986b) that the Waterberg Group is nowhere developed either above or below the Soutpansberg Group, this work shows rather that the Mogalakwena Formation is developed beneath the Wyllies Poort Formation at around 23°05.76'S; 28°53.47'E. The contact between these two formations is shown in Figure 7.37 and in greater detail in Figure 7.38, These figures show that the Wyllies Poort Formation rests above the Mogalakwena Formation on a gentle angular unconformity.

The stratigraphic relationship between the Sibasa Formation and the Mogalakwena Formation could not, however, be established. As the map in Appendix 1 shows, these two Formations are developed together only in the western foothills of Blouberg. It is possible that the Mogalakwena Formation may dip westwards beneath the Sibasa basalt (Appendix 1), though it also possible that the contact between these two formations may be faulted here rather than sedimentary (Appendix 1). The relationship between the Sibasa Formation and the overlying Wyllies Poort Formation could not be established.

7.8: Relationships formed by intrusive rocks:

Appendix 1 shows that, whilst dyke swarms cut the basement, the Blouberg, Setlaole, Makgabeng and the Mogalakwena formations, they are undetected as cutting the Sibasa Formation, and were not recorded cutting the extensive outcrops of the Wyllies Poort Formation. There is also a pattern of spatial distribution, whereby the extent of outcrops of dykes is generally restricted to the area south of the southern strand of the Melinda Fault.

Figure 7.1: Crush breccia on the southern strand of the Melinda Fault at 23°07.39'S; 28°57.46'E. Note the lack of foliation or amphibolite lenses. Camera bag is 25cm high.

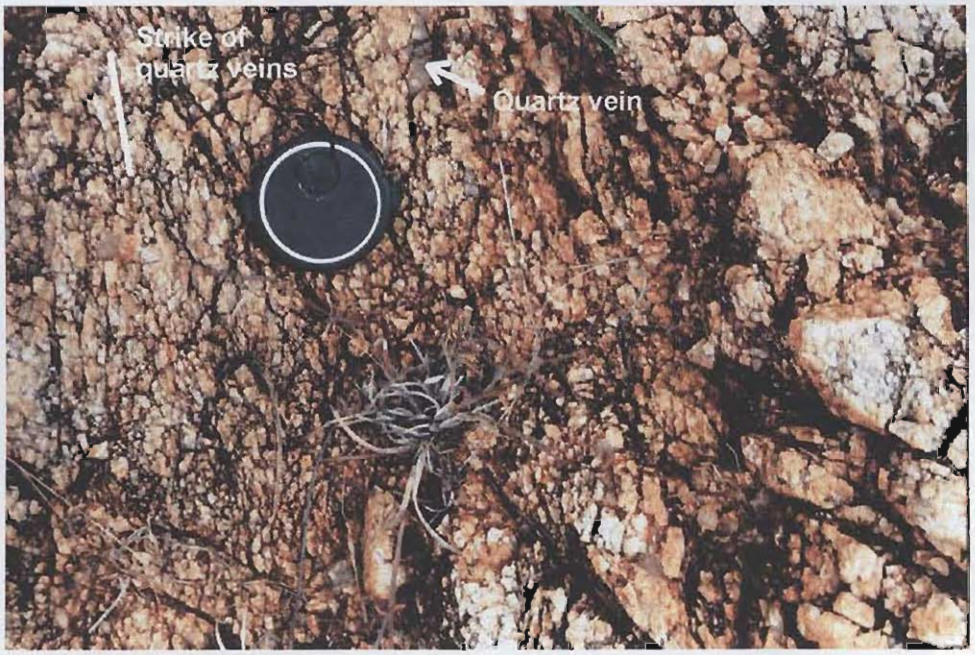

Figure 7.2: Detail of crush breccia at 23°07.39'S; 28°57.46'E. Note the lack of cohesion and presence of thin quartz veins. Lens cap is 5cm wide.

Figure 7.3: Crush breccia showing intense intrusion of quartz veins, which strike parallel to the strike of the southern strand of the Melinda Fault. Recorded at 23°07.39'S; 28°57.46'E. Lens cap is 5cm wide.

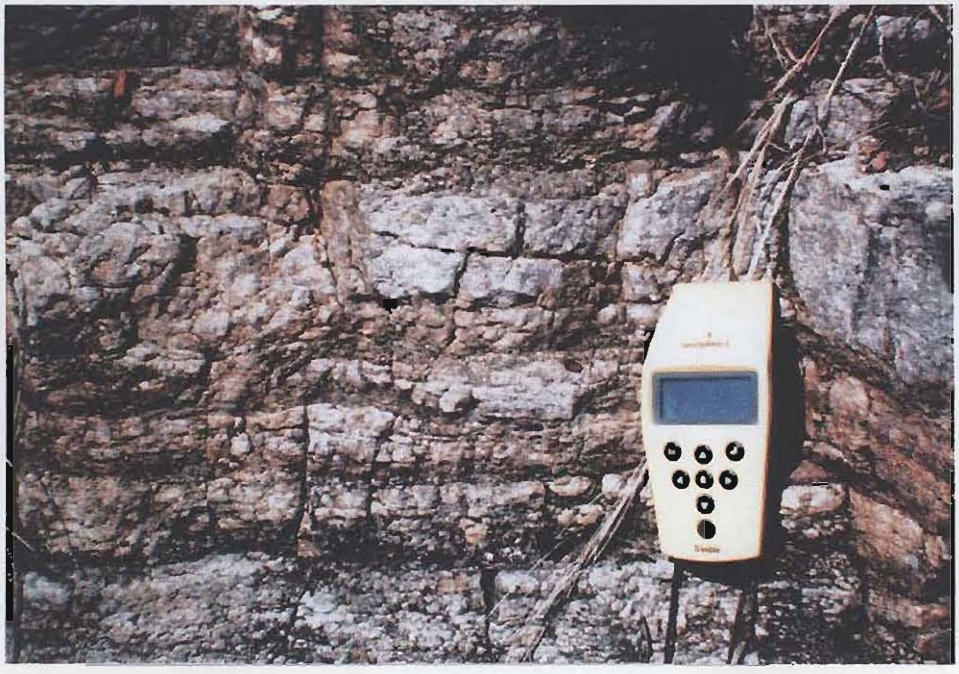

Figure 7.4: Low-angled foliation developed on a thrust fault at 23°07.17'S; 29°02.66'E. Dip-direction of thrust plane: 10°→030°. G.P.S. receiver is 15cm high.

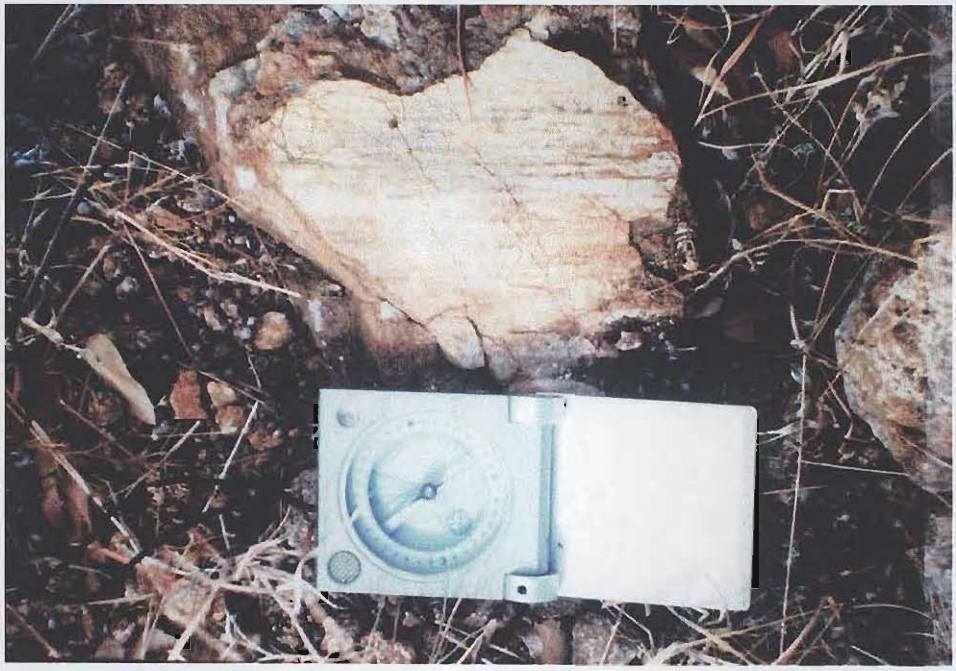

Figure 7.5: Horizontal slickensided surface caused by brittle reactivation in basement gneiss at 23°07.20'S; 29°02.92'E. The compass (7cm wide) is orientated parallel to the lineation, and shows a trend of 200°. Stepping on the surface suggests vergence towards the south.

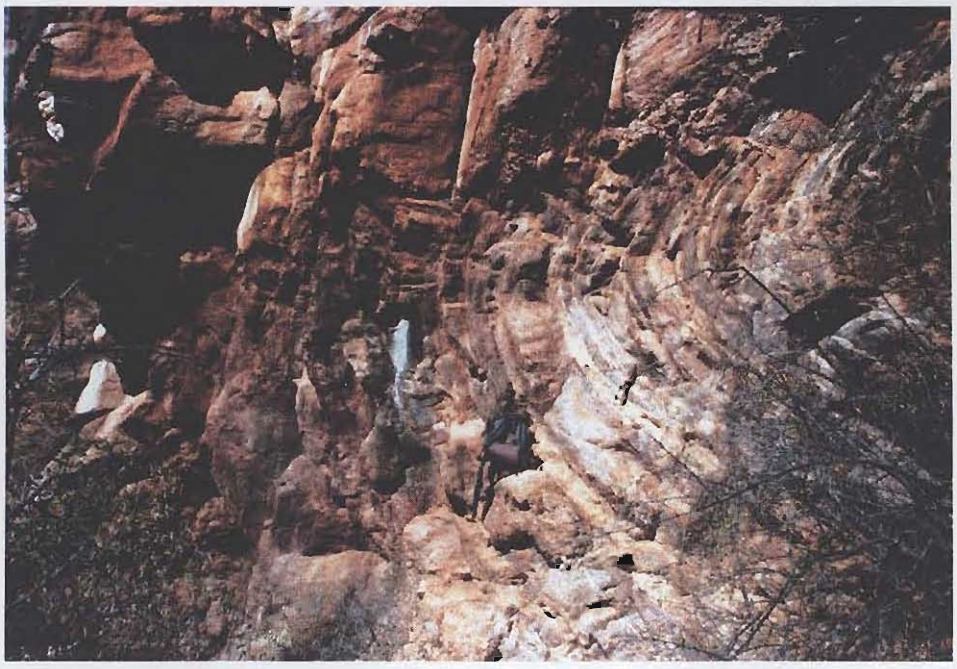

Figure 7.8: Folding developed in the Blouberg Formation at 23°05.76'S; 28°53.47'E. View is approximately eastwards, showing the east-west trending fold axis plotted in Figure 7.9. Rucksack is 50cm high.

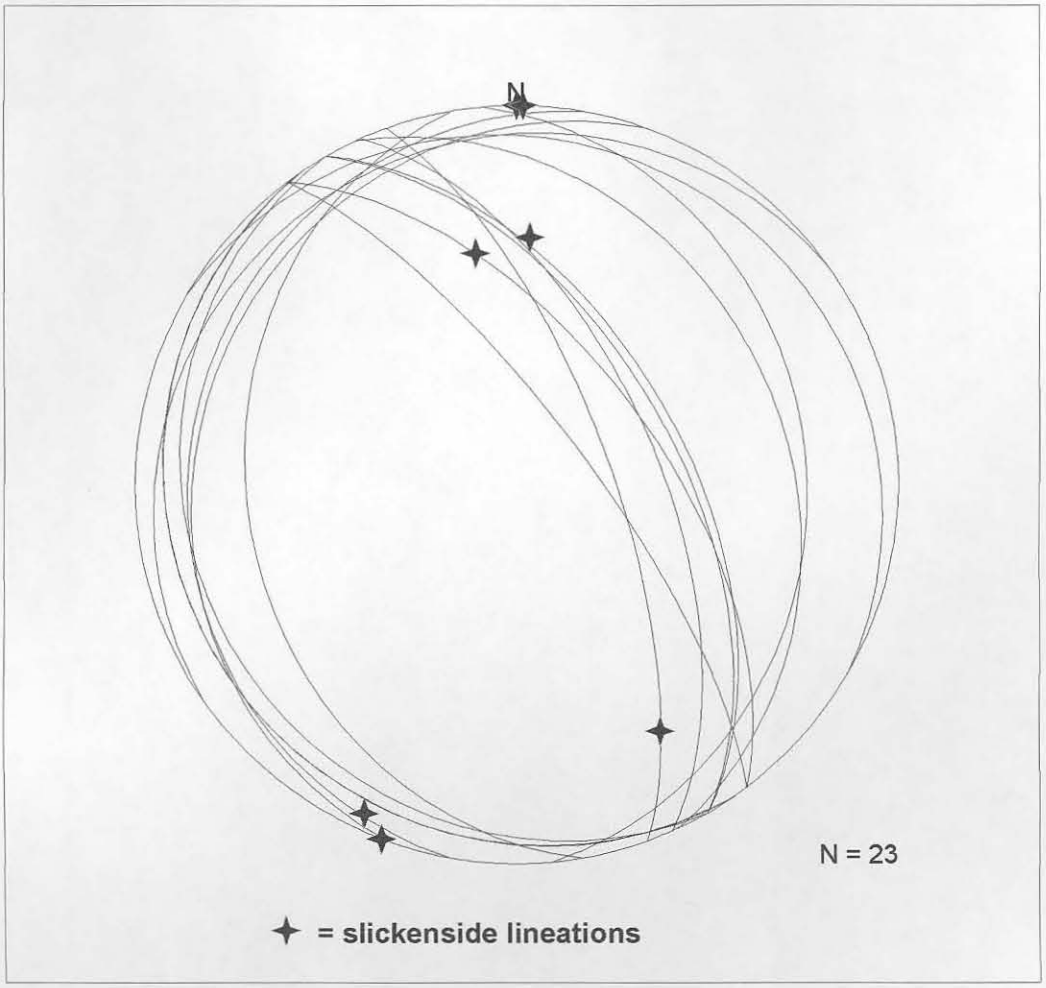

Figure 7.6: Stereographic projection showing orientation of low-angled thrust fault planes cuttingthe basement gneiss, and the orientation of slickenside lineations developed on some of those surfaces.

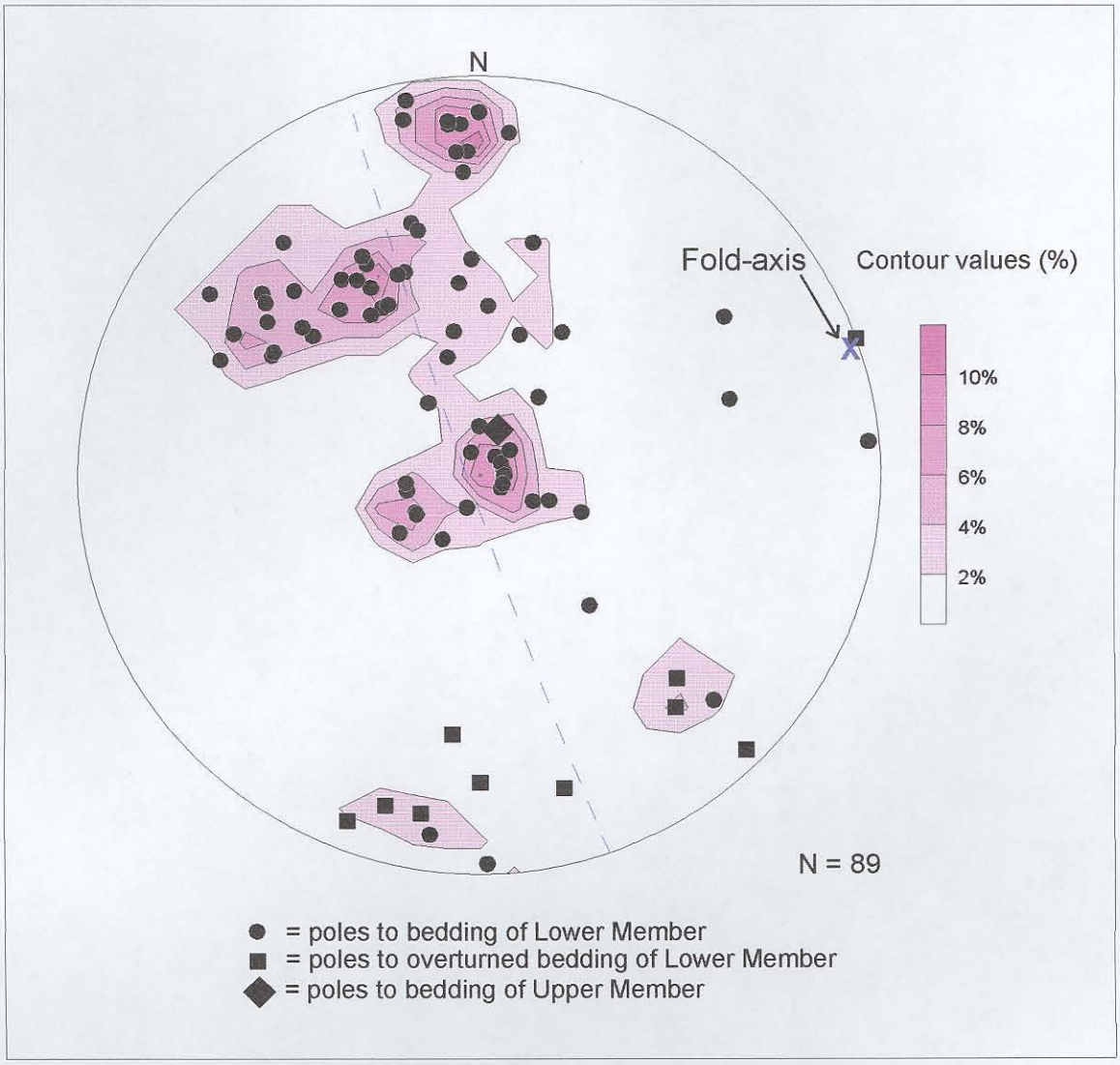

Figure 7.7: Stereographic projection showing poles to bedding planes recorded in the Blouberg Formation in the Blouberg mountain area.

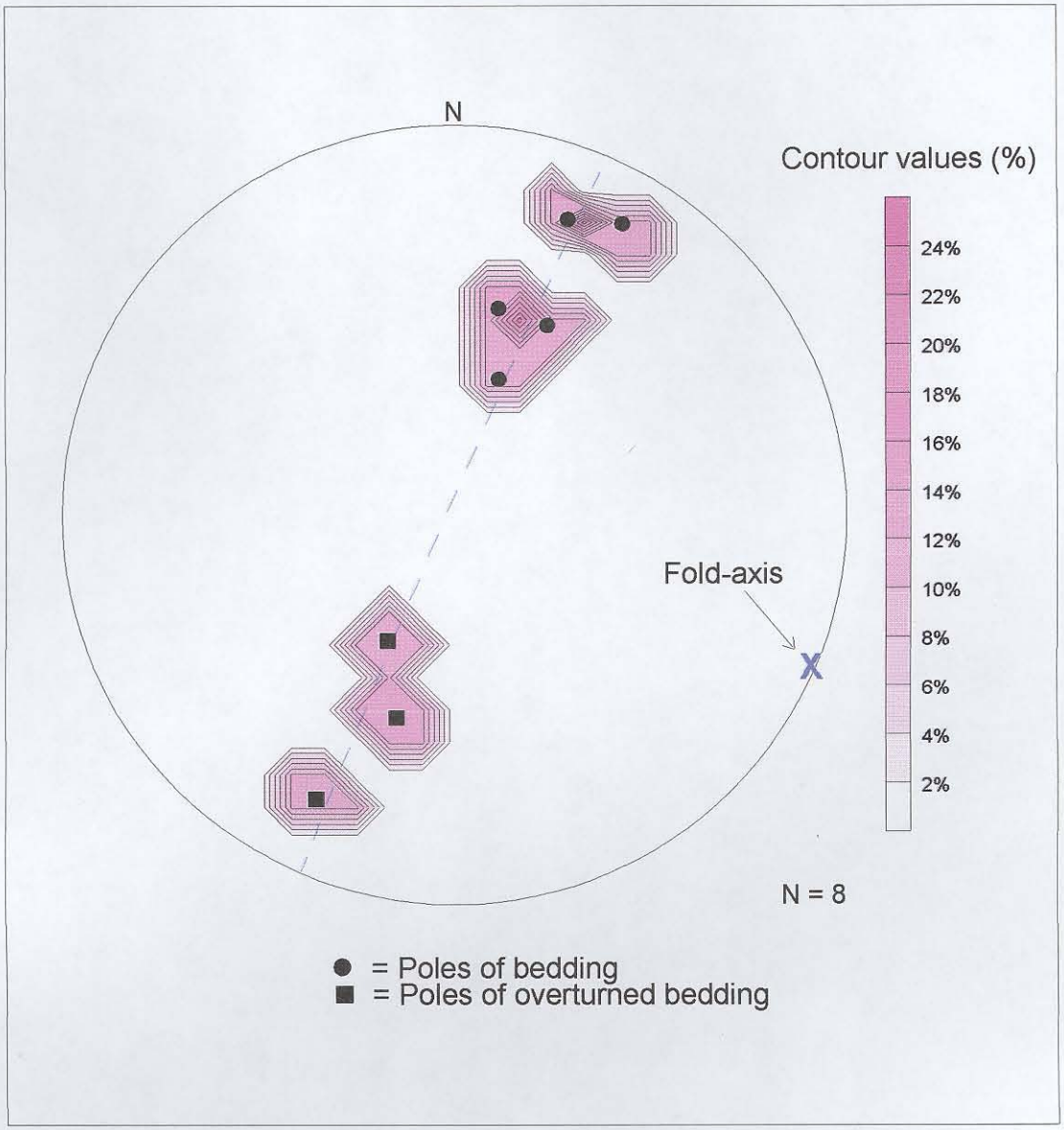

Figure 7.9: Stereographic projection showing poles to bedding planes of Blouberg strata at 23°05.76'S; 28°53.47'E.

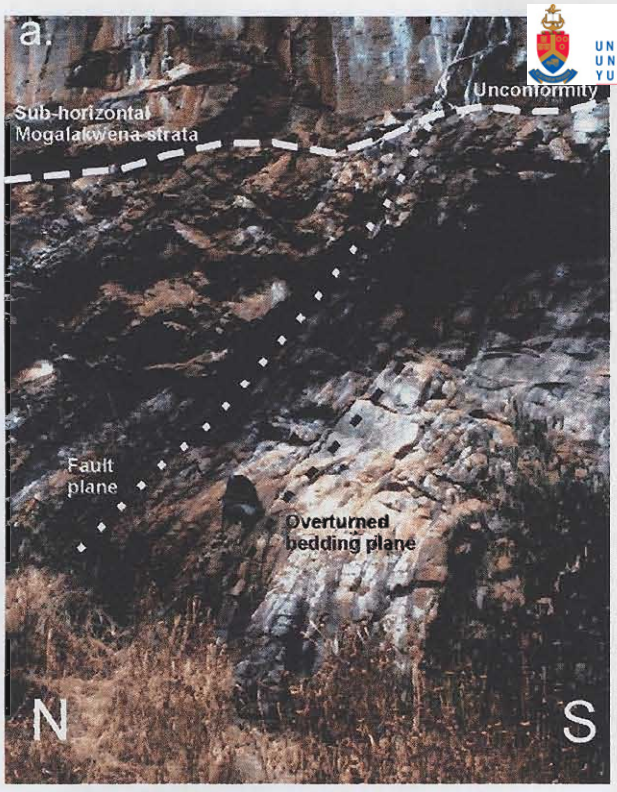

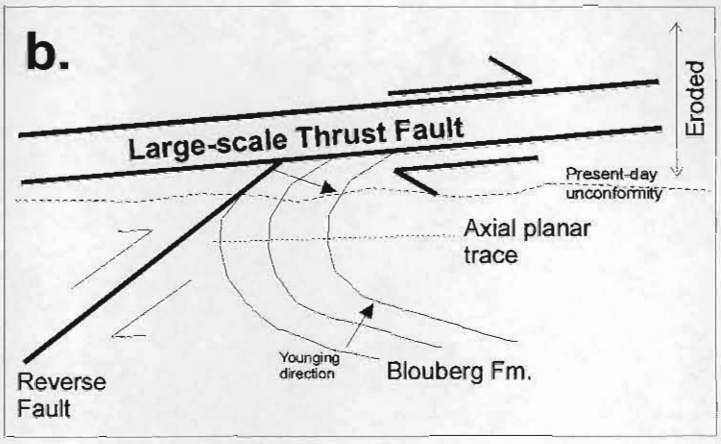

Figure 7.10a: Steeply-dipping reverse fault recorded at 23°06.70'S; 28°59.43'E, which cuts the Blouberg Formation. Fault plane has a dip-direction of 52°→004°, and slickenside lineations have an orientation of 52°→004° (i.e. dip-slip movement). Weak fabric and stepping on slickenside lineations suggest a vergence to the south. Rucksack is 50cm high.

Figure 7.10b: Folded and overturned bedding and reverse fault can be explained by the inferred presence of large-scale southwards-vergent thrust fault above ach portion of overturned bedding.

Figure 7.12: Slickenside lineations developed in the Blouberg Formation at 23°07.96'S; 28°55.25'E. Dip-direction of fault plane is 05°→228°, and slickenside lineations are orientated 0°→180°. Stepping suggests vergence towards the south. Compass (7cm wide) is orientated north.

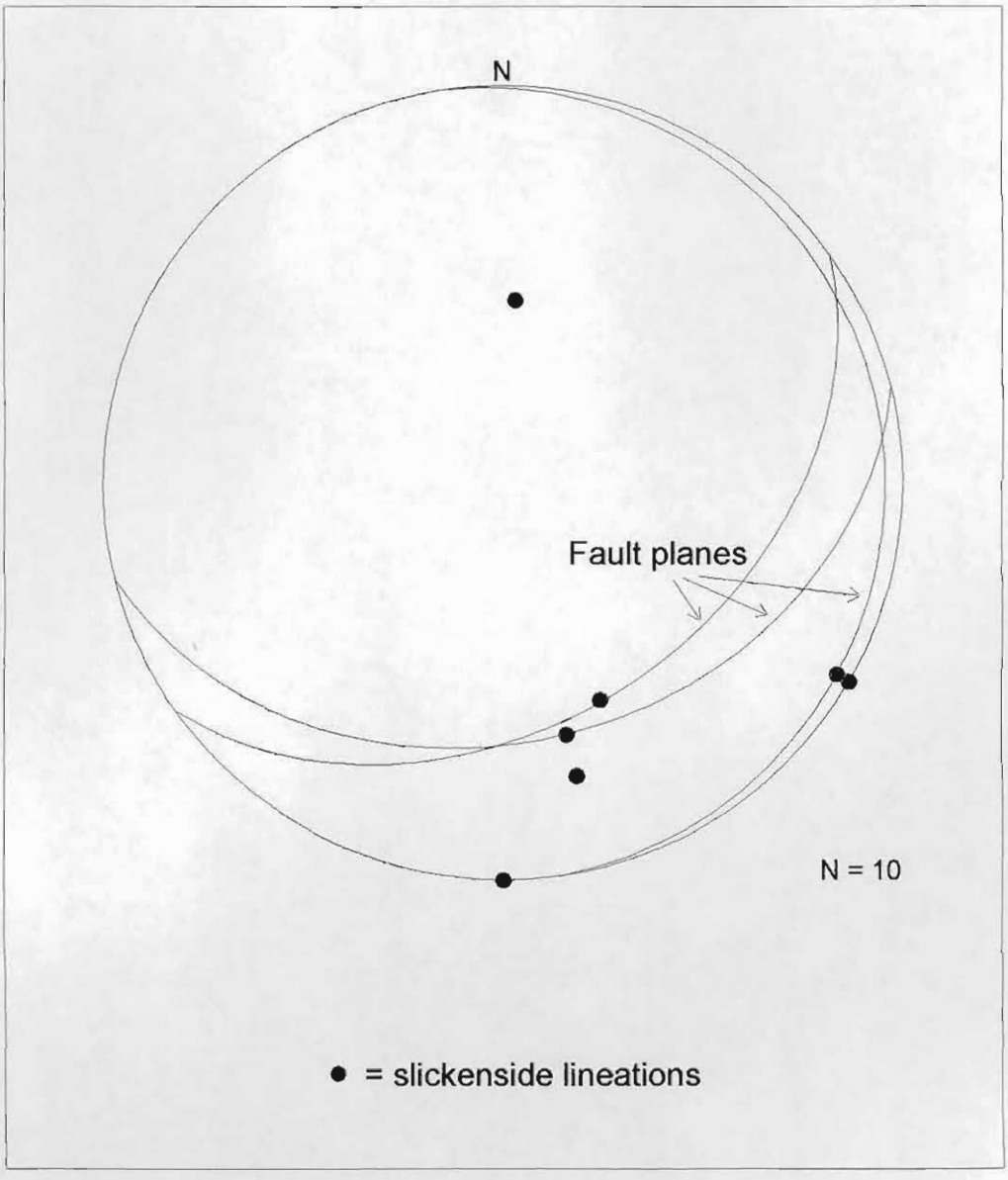

Figure 7.11: Stereographic projection showing the orientation of slickenside lineations and some associated fault planes in the Blouberg Formation.

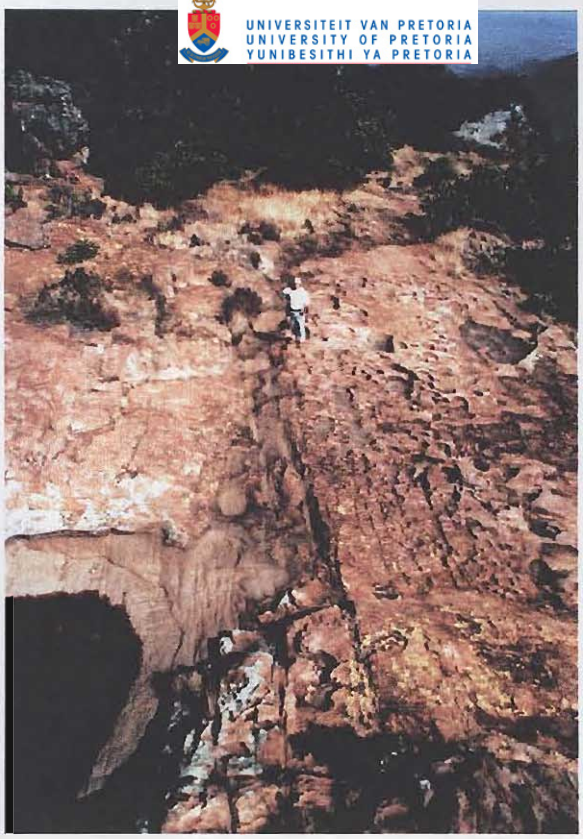

Figure 7.13: Intense jointing in the lower Wyllies Poort Formation at 23°04.99'S; 28°59.33'E. Joints strike 010°. View looking south.

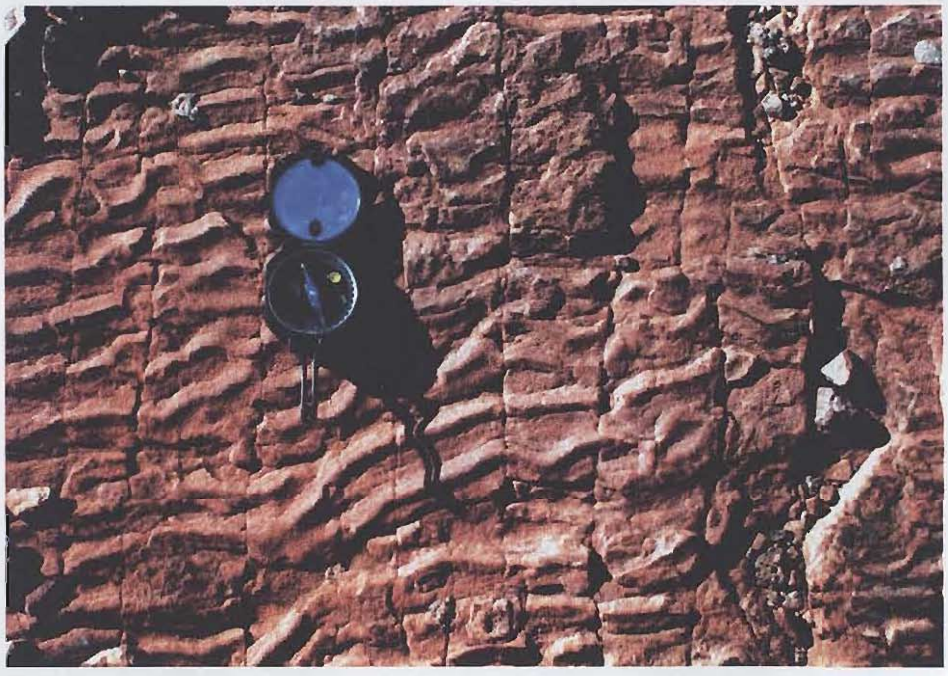

Figure 7.14: 010°-striking joint planes developed in the asymmetric rippled planar bedding of the upper Wyllies Poort Formation at 23°04.22'S; 28°59.38'E (summit of Blouberg mountain). Compass is 6cm wide.

Figure 7.15: Fault developed in the lower strata of the Wyllies Poort Formation at 23°04.99'S; 28°59.33'E. Fault plane strikes 285°, and fabric suggests dextral strike-slip displacement. Needle of compass (7cm wide) points to north.

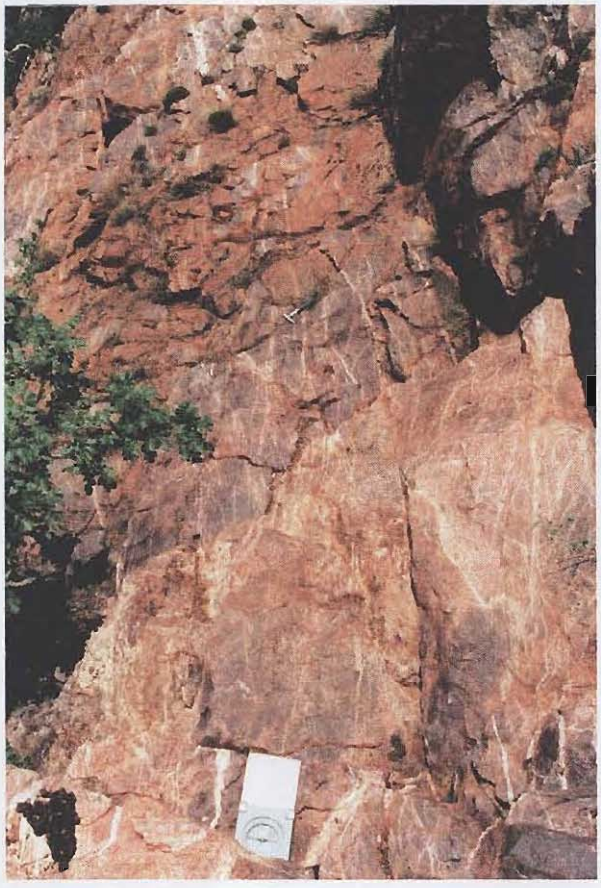

Figure 7.18: Quartz-filled veins intruding the Wyllies Poort Formation at 23°00.93'S; 28°02.88'E. Veins strike 100°. Needle of compass (7cm wide) points north, and hammer (in middle ground) is 30cm long.

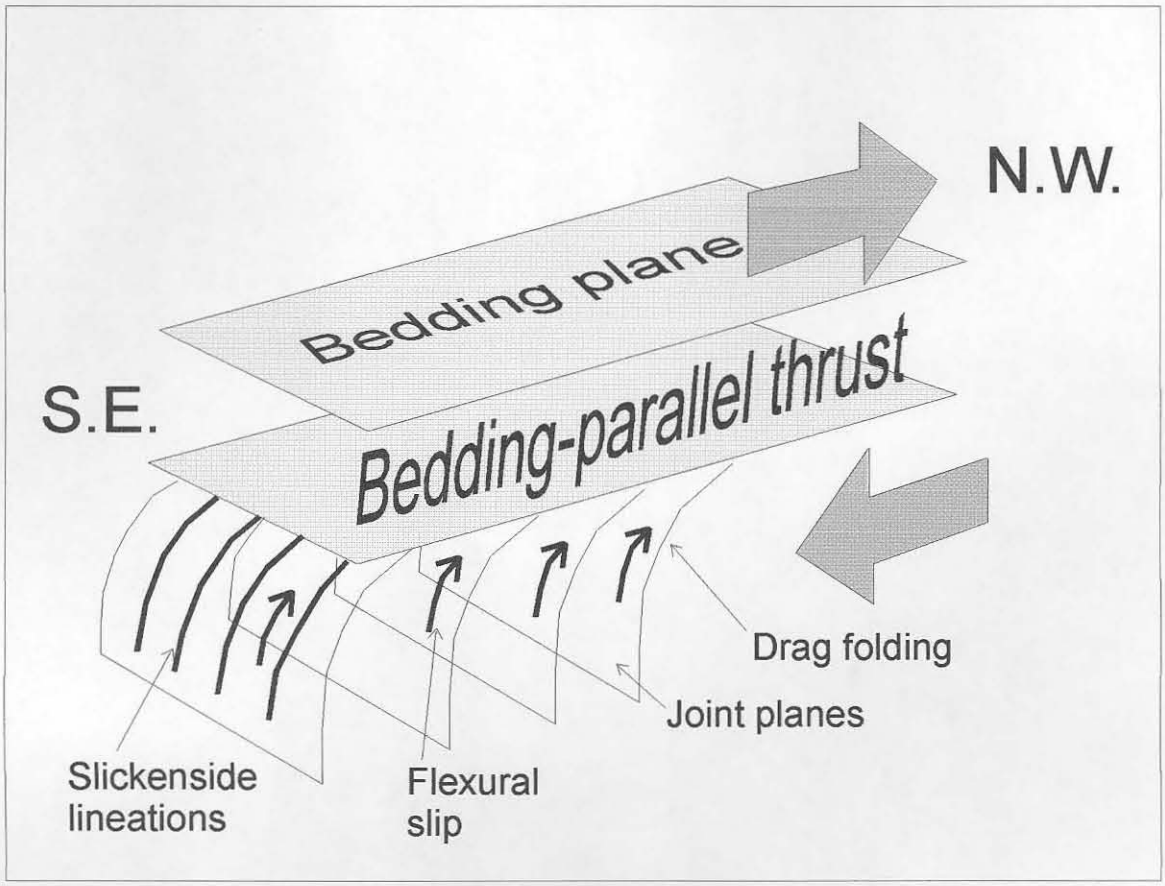

Figure 7.16: Sketch showing relationship between bedding-parallel thrust, folded joint planes, and slickenside lineations recorded at 23° 04.69'S; 28° 59.49'E.

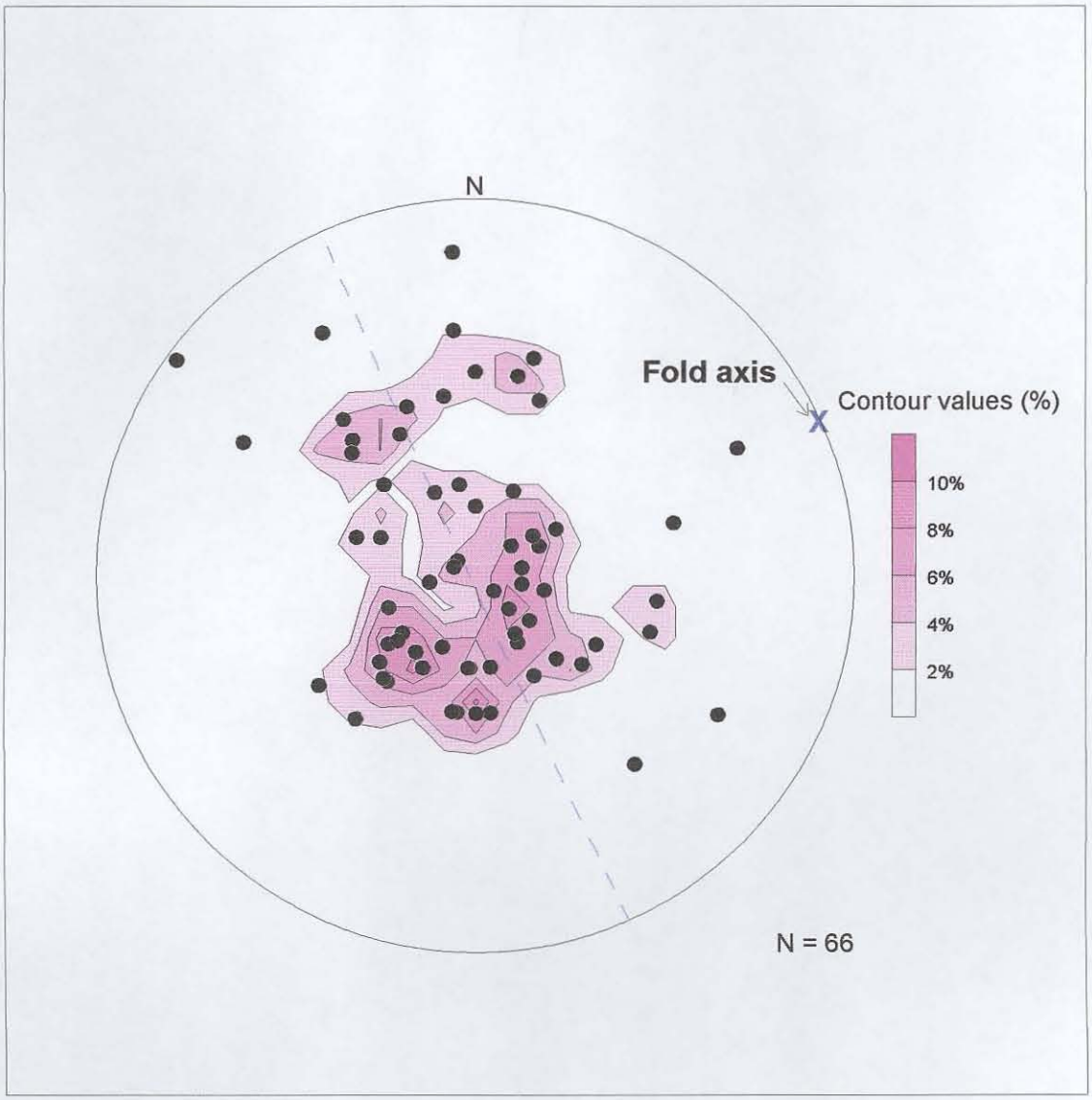

Figure 7.17: Stereographic projection showing the poles to bedding planes in the Wyllies Poort Formation in the vicinity of the northern strand of the Melinda Fault. Fold axis (01°→ 066°) is shown.

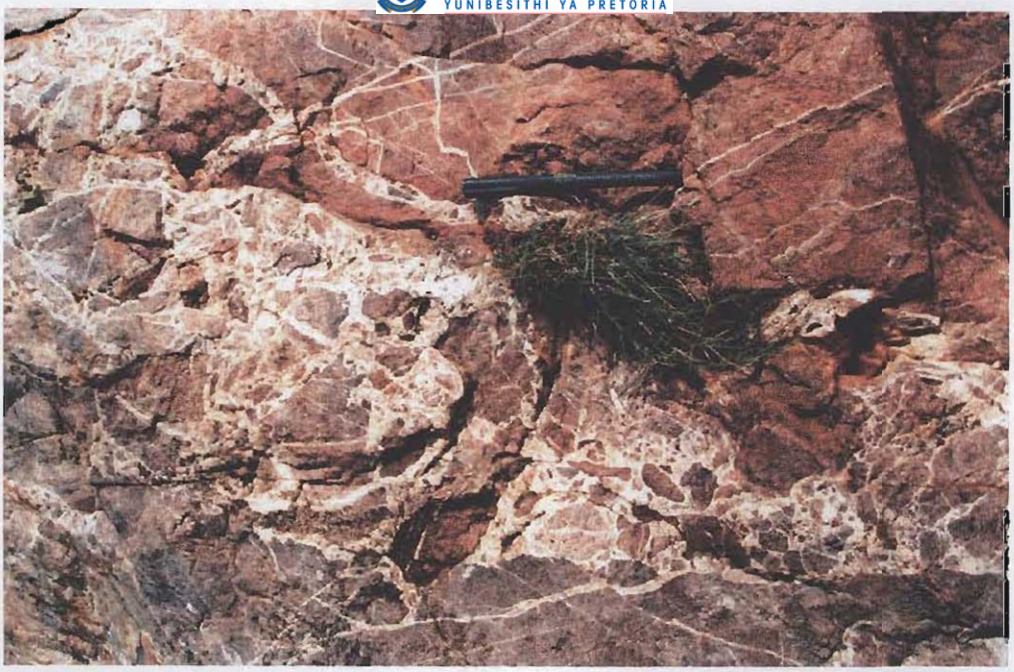

Figure 7.19: Quartz-filled veins intruding an early brittle fault in the Wyllies Poort Formation at 23°00.93'S; 28°02.88'E. Pen is 15cm long.

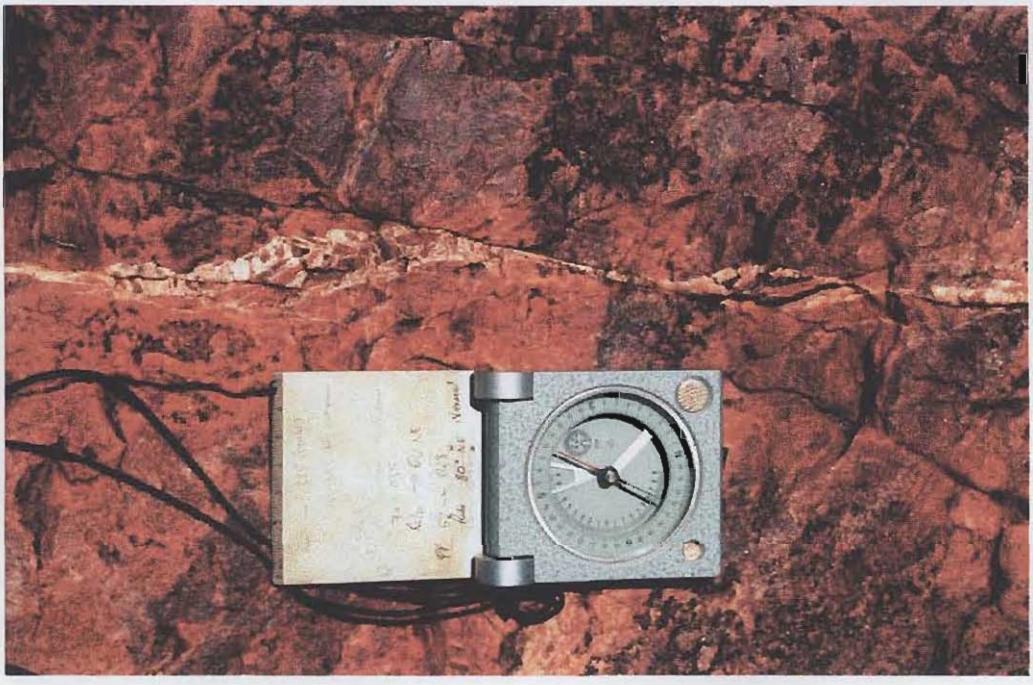

Figure 7.20: 140°-striking sinistral dilatational vein (displacement c. 2cm) at 23°01.34'S; 28°04.45'E. Needle of compass (7cm wide) points north.

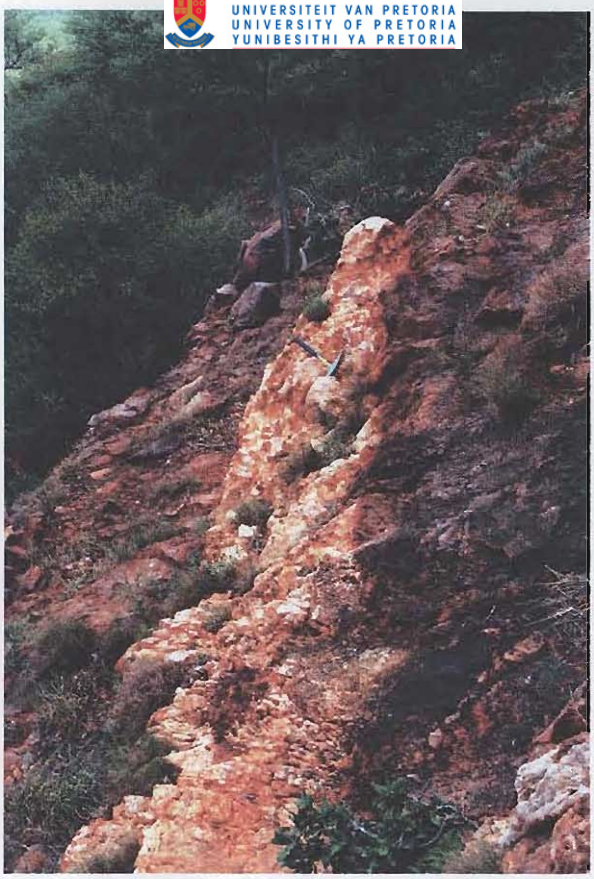

Figure 7.21: 1.5m wide quartz-filled vein cutting the Wyllies Poort Formation at 23°00.51'S; 28°07.71'E. Hammer is 30cm long.

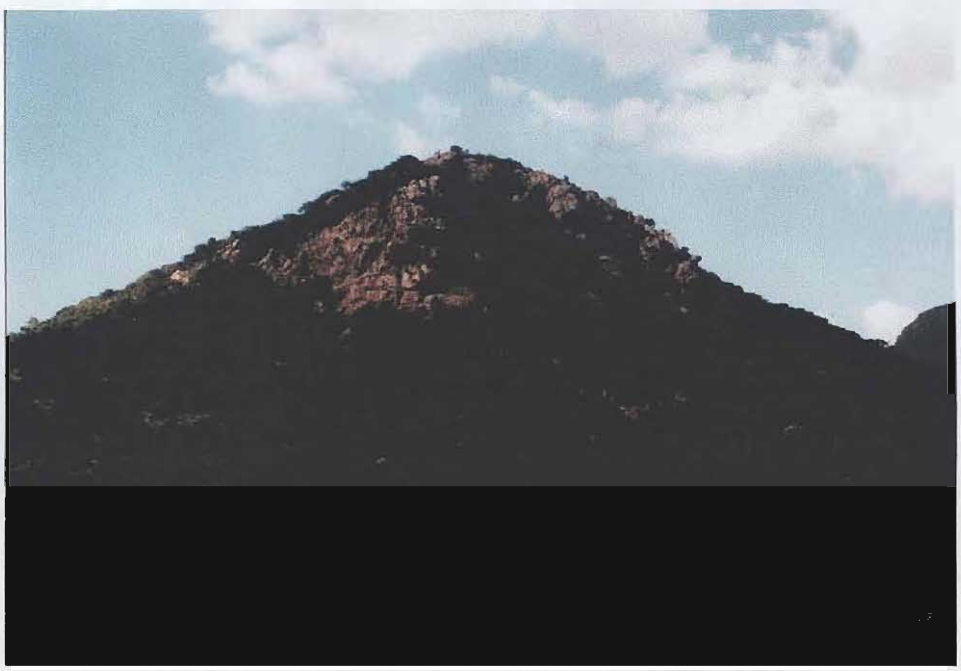

Figure 7.22: Small hill at 23°03.02'S; 28°56.38'E composed of white quartzite. The northern strand of the Melinda Fault is thought to underlie this area (Appendix 1).

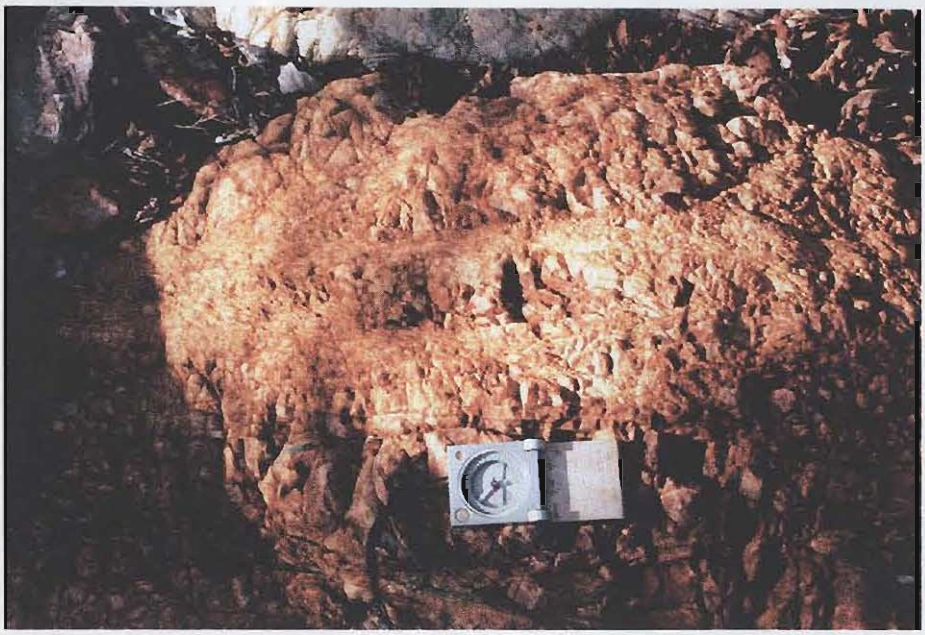

Figure 7.23: East-west striking fault breccia cutting the Wyllies Poort Formation at 23°02.50'S; 29°04.10'E. Needle of Compass (7cm wide) points north.

Figure 7.24: Fault plane with a dip-direction of 74°→033° at 23°01.23'S; 28°02.07'E, with fault breccia preserved on the fault plane. Pen is 15cm long.

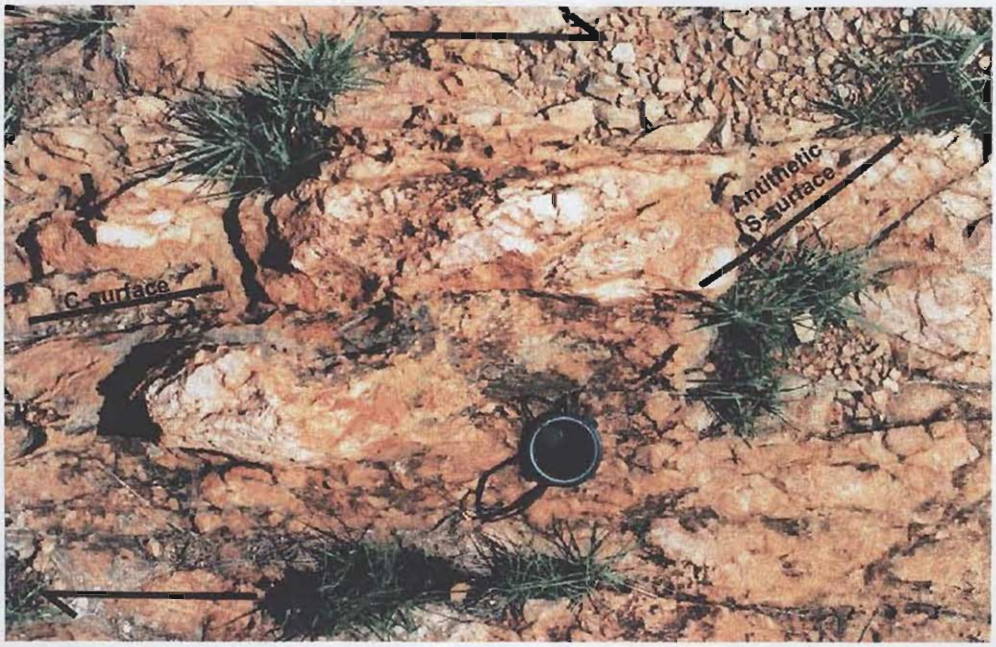

Figure 7.25: Fault breccia at 23°01.31'S; 28°04.65'E, with a weak S-C fabric which suggests dextral displacement. Lens cap is 5cm wide.

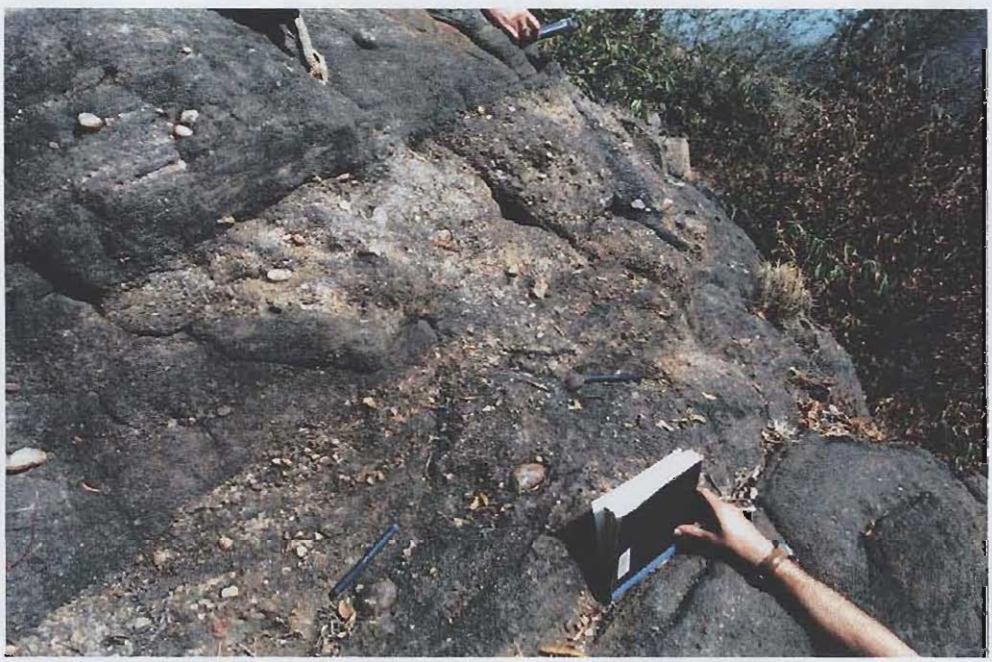

Figure 7.30: Pronounced angular unconformity between the overturned Blouberg Formation (bedding plane indicated by lower notebook) and the Mogalakwena Formation above (bedding plane indicated by upper notebook). Recorded at 23°07.35'S; 28°57.53'E.

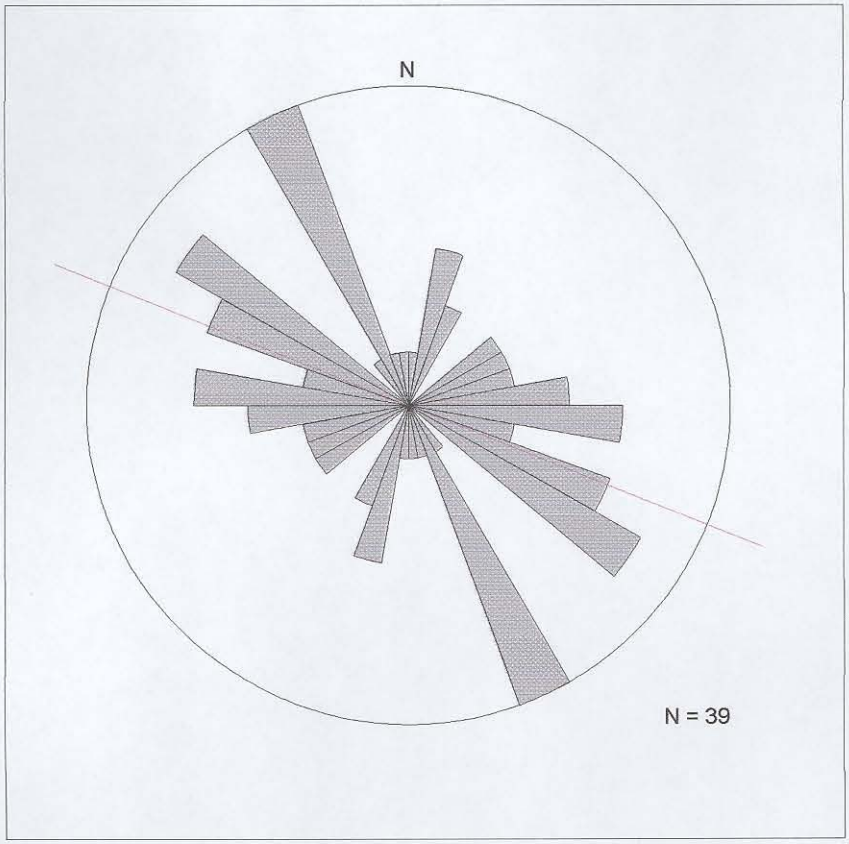

Figure 7.26: Rose diagram showing the strike of joints in the Wyllies Poort Formation. Principal trend is shown.

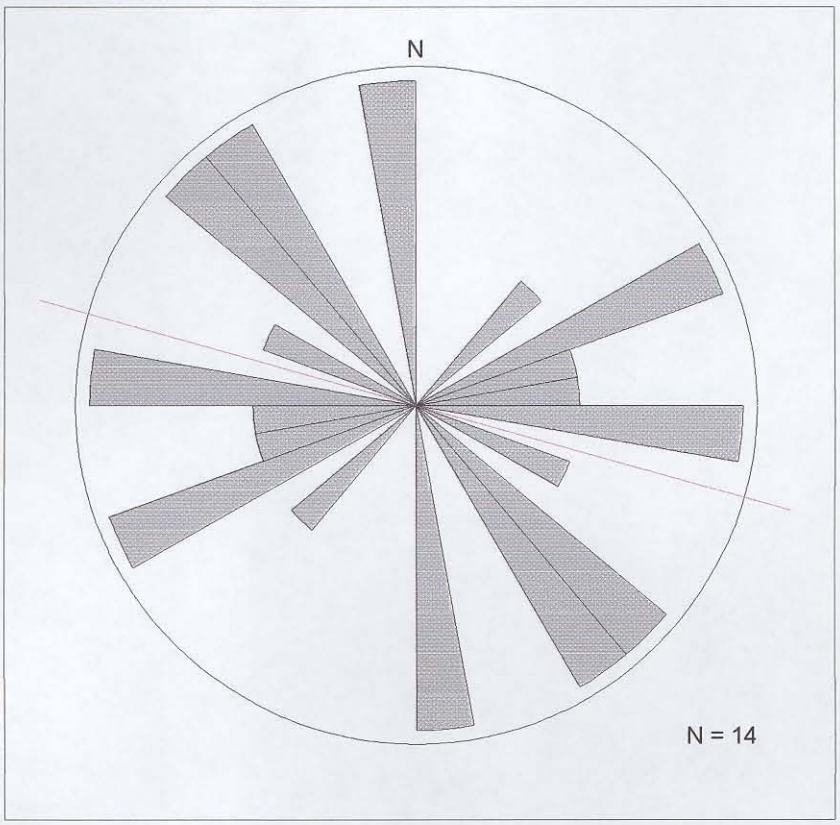

Figure 7.27: Rose diagram to show the strike of veins cutting the Wyllies Poort Formation. Principal trend is shown.

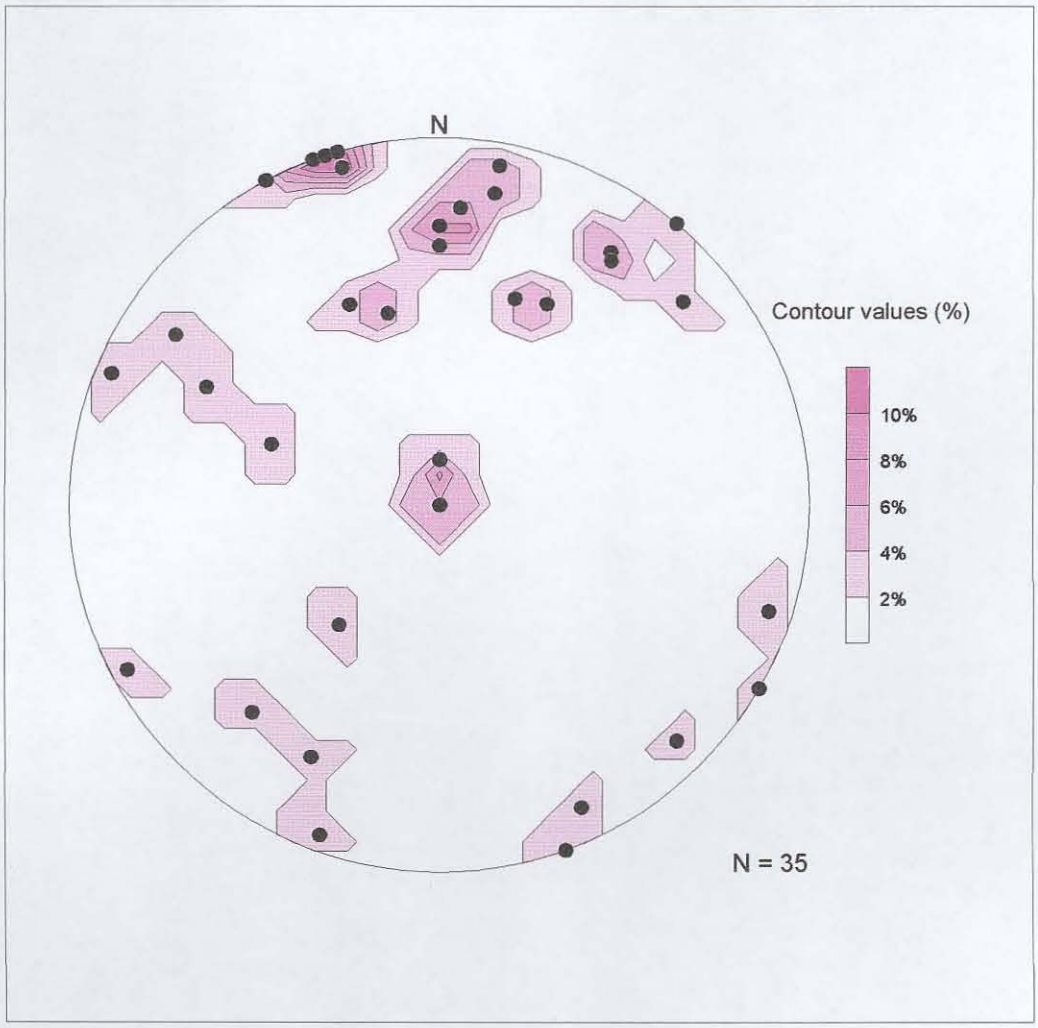

Figure 7.28: Stereographic projection of poles to fault planes in the Wyllies Poort Formation (associated slickensides are potted in Figure 7.29).

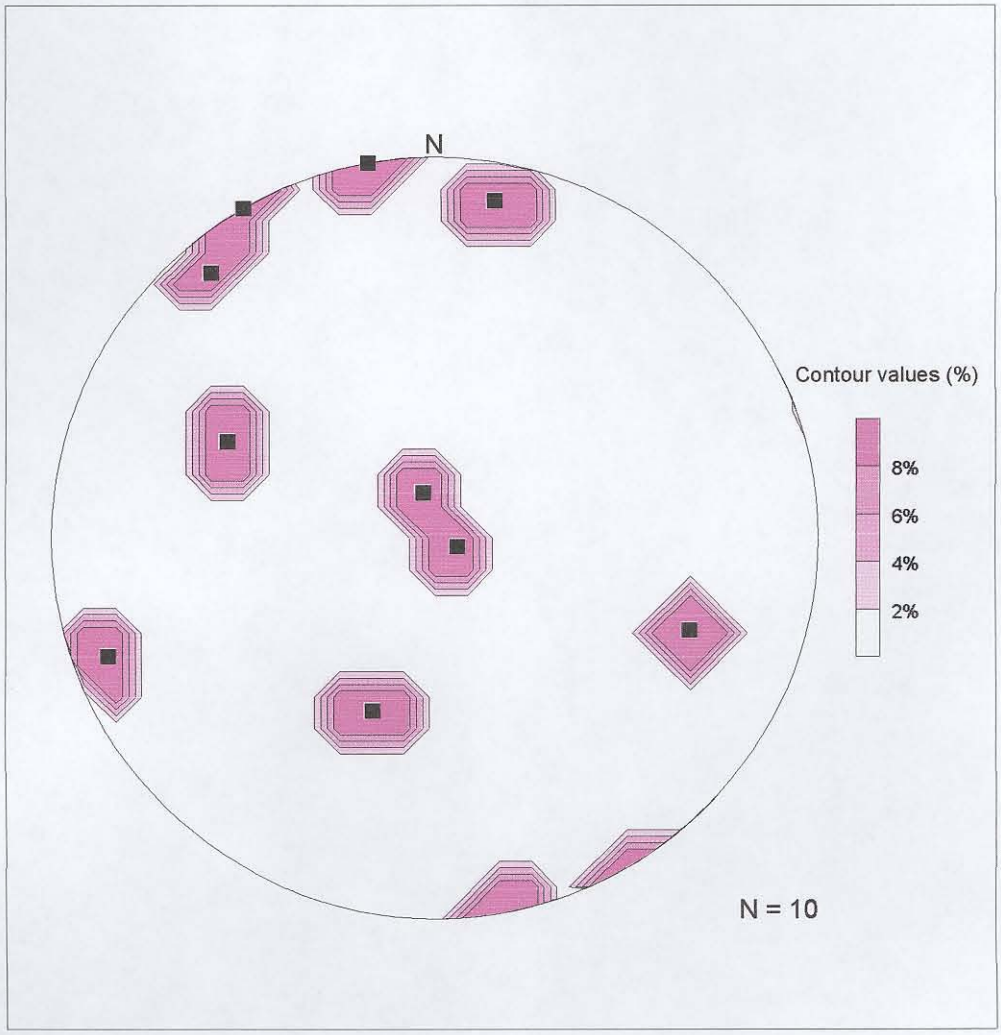

Figure 7.29: Stereographic projection showing the orientation of slickenside lineations (associated with fault planes in Figure 7.28) in the Wyllies Poort Formation.

Figure 7.31: Pronounced angular unconformity between the folded and locally overturned Blouberg Formation and the Mogalakwena Formation above. Recorded at 23°06.80'S; 28°59.40.'E. Note the 1m deep channel developed on the upper surface of the Blouberg Formation to the left of the hammer (30cm long). View taken looking east.

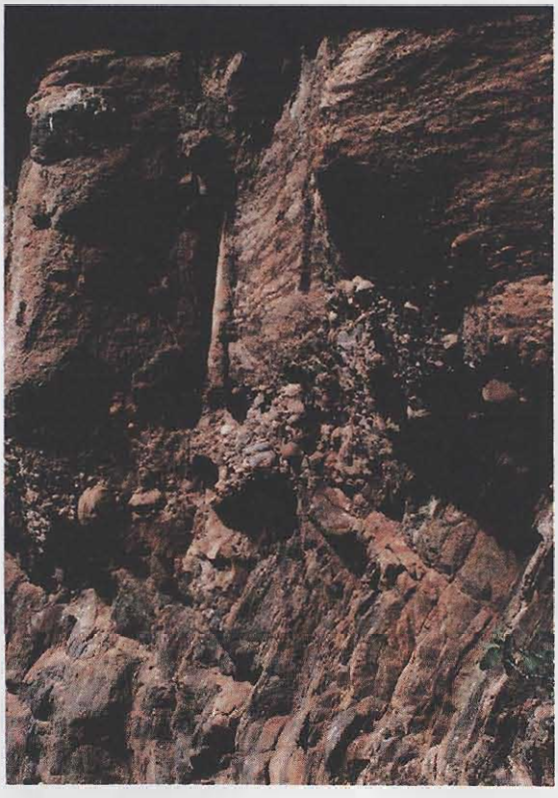

Figure 7.32: Pronounced angular unconformity between the overturned Blouberg Formation and the Mogalakwena Formation above, marked by thin basal conglomerate. Recorded at 23°05.76'S; 28°53.47'E. Cliff section is c. 2m high.

Figure 7.33: Disconformity (or slight angular unconformity) developed between the Makgabeng Formation (laminated medium-grained sandstone) and the Mogalakwena Formation (cobbles and coarse sandstone). Recorded at 23°11.23'S; 28°52.44'E. Lens cap is 5cm wide.

Figure 7.34: Disconformity (or unconformity) between the Makgabeng Formation (with well-developed joint planes) and the Mogalakwena Formation (with no joint planes). Recorded at 23°16.39'S; 28°52.57'E. Large pebble in Mogalakwena Formation is 6cm long.

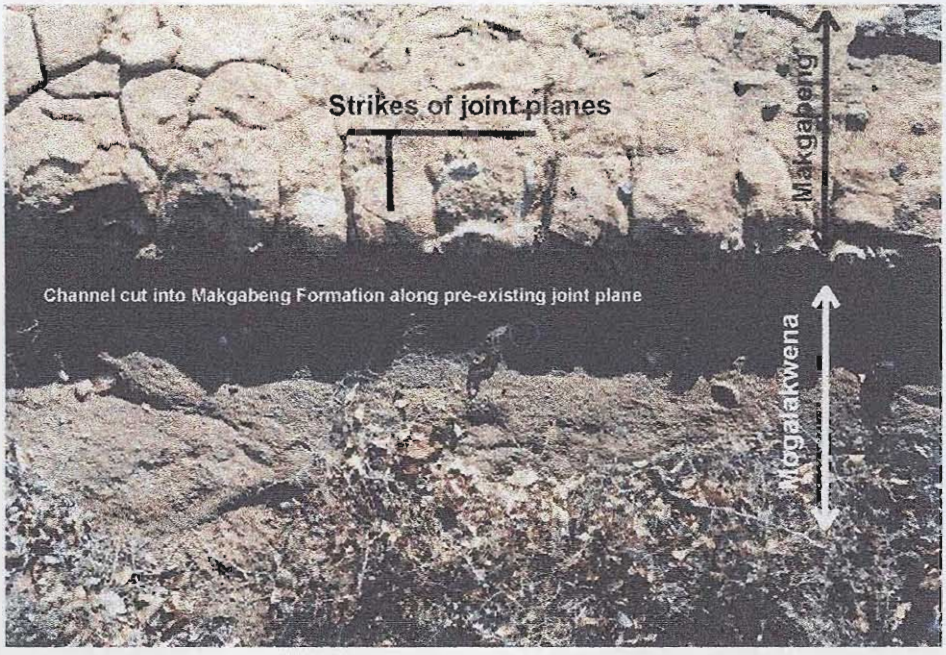

Figure 7.35: Joint plane in the Makgabeng Formation is exploited as a channel during deposition of the Mogalakwena Formation. Note that joint planes in the Makgabeng Formation are not continuous in the Mogalakwena Formation. Recorded at 23°16.39'S; 28°52.57'E. View is vertical. Lens cap is 5cm wide.

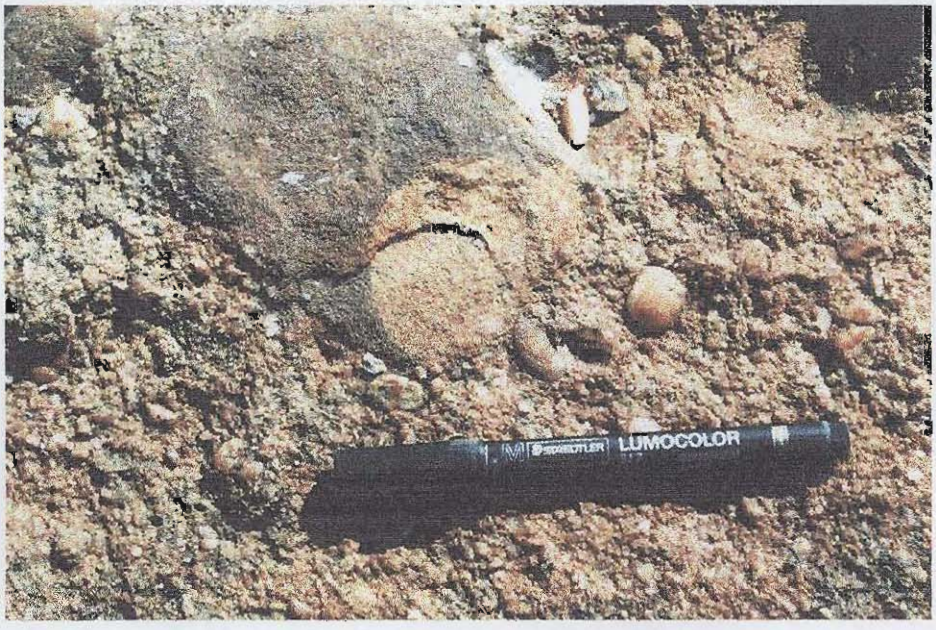

Figure 7.36: Reduction spot in the upper surface of a small inlier of the Makgabeng Formation is not continuous into coarse grained strata of the Mogalakwena Formation, indicating the onset of diagenetic processes prior to deposition of the Mogalakwena Formation. Recorded at 23°16.39'S; 28°52.57'E. Pen is 15 cm long.

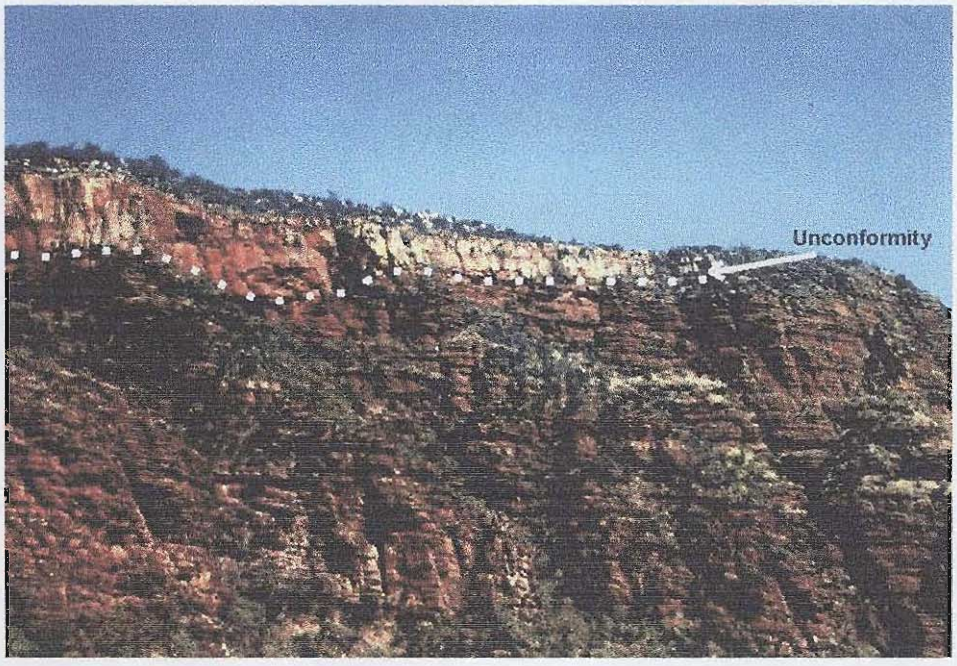

Figure 7.37: Gentle angular unconformity developed between the Mogalakwena Formation and the Wyllies Poort Formation above. Recorded at 23°05.76'S; 28°53.47'E. Cliff section is 100m high.

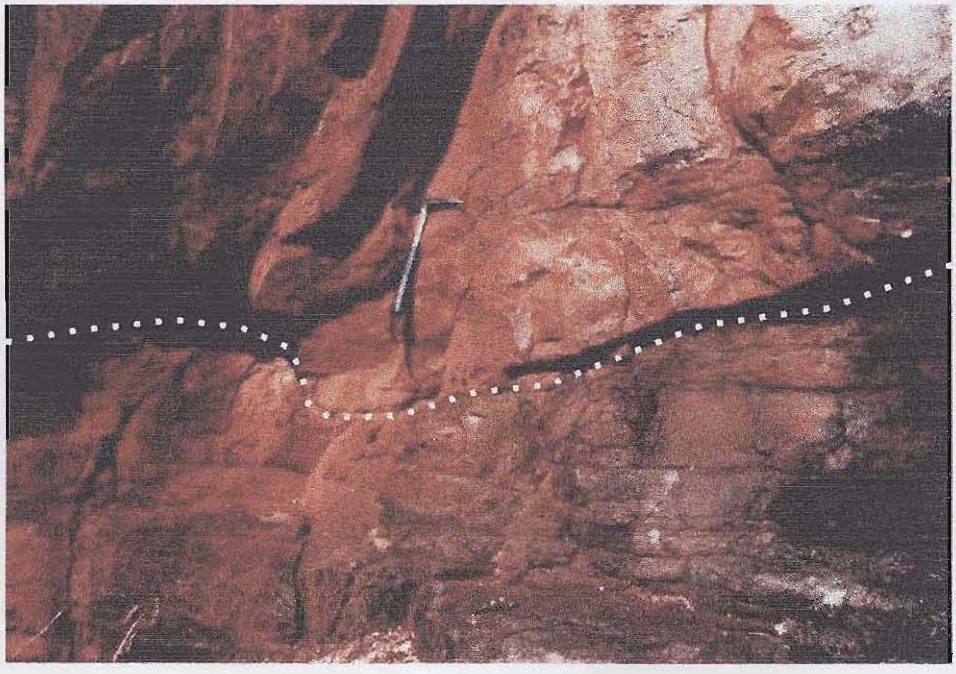

Figure 7.38: Detail of the gentle angular unconformity between the Mogalakwena Formation and the Wyllies Poort Formation above. Recorded at 23°05.76'S; 28°53.47'E. Hammer is 30cm long.